In Situ Polymerization of *N*,*N*-Dimethylacrylamide in Aerosol OT−Water: Modified Lamellar Structure and Multiphase Separation

I. E. Pacios,*,† C. S. Renamayor,† A. Horta,† B. Lindman,‡ and K. Thuresson‡

CC. y TT. Fisicoquímicas, Facultad de Ciencias, UNED, P° Senda del Rey, 9, 28040 Madrid, Spain, and Physical Chemistry 1, Center for Chemistry and Chemical Engineering, Lund University, P.O. Box 124, SSE-2211 00 Lund, Sweden

Received May 13, 2002; Revised Manuscript Received July 30, 2002

ABSTRACT: *N*,*N*-Dimethylacrylamide is polymerized in the lyotropic surfactant system containing Aerosol-OT (AOT) and water. The polymerization is thermally initiated with AIBN, which allows a homogeneous initiation in this very viscous mixture. The starting mixture contains a lamellar liquid crystalline phase and an isotropic phase in equilibrium. After the polymerization, new phases develop which appear to have a lamellar structure, even if originated from the initial isotropic phase. More phases appear after the polymerization, and they are lamellar, since the phase behavior shifts toward the lamellar region when the monomer is consumed. Once the polymer is formed *in situ*, it segregates from the lamellae and forms an isotropic microphase which does not macroscopically separate. The appearance of this polymer-rich phase modifies the structure of the lamellar mesophase by partially deswelling it. This gives a shorter lamellar spacing. The law that expresses how the AOT−H_2O spacing is contracted by the polymer is deduced from the equilibrium between the two (lamellar and isotropic) microphases. All the macroscopic final phases contain polymer, although in different proportions. The molecular weight of the polymer is the same in all phases. The presence of AOT in the medium has no influence on the resulting tacticity, which is the same as that for a polymer obtained in pure water.

Introduction

Conventional polymerization processes yield materials which, in general, have no supramolecular order, with the exception of polymer liquid crystals. However, recently, one of the interests of polymer science has been the obtainment of nanostructured "common" polymers. From this perspective, the research activity has been directed toward the obtainment of polymeric copies of thermotropic[1] or lyotropic mesophases.[2] Lyotropic liquid crystals usually consist of an amphiphile and an aqueous solvent, which in certain ranges of concentration produce an ordered or repeated structure on the nanometer size scale. This brings the possibility of using such structures as templates during the polymerization, to obtain materials useful for technological applications, such as nanocomposites, materials for controlled release, membranes, and so forth.

Aiming at obtaining polymer nanoparticles, a lot of work has been published about polymerization in microemulsion[3] or inverse emulsion[4] surfactant phases, but only a few studies report on the polymerization in other mesophases such as hexagonal, cubic, or lamellar[5−7] ones. Considerable difficulties arise in templating liquid crystal structures in polymers, because it is unfavorable to confine polymers in small dimensions and because segregation often occurs.[8] Nevertheless, the separation process could yield nanostructures, as a result of the phase-separation process rather than from liquid crystalline arrays.[9]

Pioneering studies were performed in un-cross-linked polymers,[10−12] but the results were not promising, since the initial order was lost in the polymerization. Tests were then made to cross-link the polymer to obtain three-dimensional ordered polymer networks, in the ideal case as a cast of the supramolecular structure, and this is actually the subject of most of the research.[9,13,14] Only in the last two years has the objective of obtaining templated linear polymers been reconsidered, and the polymerization of un-cross-linked polystyrene in a lamellar or cubic lyotropic mesophase has been studied.[6,7] In this system, the structure is maintained, but a phase-separation occurs between the polymer and the amphiphile.

When polymers are synthesized in a nanostructured system, as a lyotropic mesophase, the medium can modify characteristics such as molecular weight[15] and polymerization kinetics.[16] On the other hand, the polymerization reaction can also modify the lyotropic structures of the mesophase.[17]

In the present paper, we report on the polymerization of a water-soluble monomer (*N*,*N*-dimethylacrylamide, DMAA) in a lyotropic medium (AOT−water) which forms a lamellar liquid crystalline mesophase. We aim at determining the changes in the mesophase structure which are induced by the polymerization process and at detecting if any template effect has been obtained by the mesophase on the synthesized polymer. As we shall see, the synthesis of a polymer produces a contraction of the spacing in the lamellar structure of the surfactant medium, but the polymer is not affected by the mesophase.

To have a lamellar phase for the polymerization, relatively high AOT concentrations must be used (for AOT−water at 25 °C, the system is lamellar only above 15 wt % AOT; see Figure 1). At these high AOT contents, the mixtures are very viscous, and it is difficult to homogeneously disperse an added component. Stirring does not help, because of the antithixotropic behavior of AOT−water.[19] The polymerization at temperatures close to ambient is usually activated by two-component initiators which produce radicals when the two reactants are mixed. With the difficulties of attain-

† UNED.
‡ Lund University.

10.1021/ma020724q CCC: $22.00
Published on Web 08/29/2002

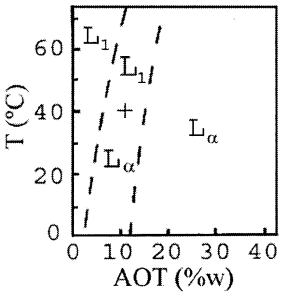

Figure 1. AOT−water phase diagram showing the regions of stability or coexistence of the lamellar (L_α) and isotropic (L_1) phases in the vicinity of the AOT concentration used here (data from ref 18).

ing good mixing in the present system, this type of initiation should lead to inhomogeneous polymerization and possibly a low yield. Therefore, a photoinitiator may be a better choice, since the latter can be thoroughly mixed before any reaction takes place and, then, activated by light at room temperature. However, photoinitiation usually requires working with thin films. In the present case, the system separates into several macroscopic phases after polymerization, and the compositions of those phases with regard to AOT, water, and polymer have to be analyzed, so the volumes of the phases have to be large enough. For these reasons, photoinitiation was not considered convenient, and a thermally activated initiator (AIBN) was chosen instead. At room temperature the latter can be homogeneously dispersed, and then, the beginning of the polymerization can be triggered in the whole sample volume at the same time simply by raising the temperature above a given threshold (60 °C).

Experimental Section

Materials. The AOT (1,4-bis(2-ethylhexyl)sodium sulfosuccinate) and *N*,*N*-dimethylacrylamide (99% purity) were obtained from Sigma and Aldrich, respectively, and both were used as received. The initiator was AIBN (α,α′-azobis(isobutyronitrile), obtained from Fluka and recrystallized from methanol. The solvent was water of reactivity quality (Milli-Q).

NMR Measurements. ^{1}H NMR spectra were recorded on a Bruker AC 200 at 200 MHz, and ^{13}C spectra were performed in a Bruker Avance DRY at 400 MHz, at 37 °C in deuterated DMSO. DEPT spectra (distortionless enhancement by polarization transfer) of PDMAA were obtained at standard conditions, and a value of the CH coupling constant $J_{CH} = 130$ Hz was considered.[20] To obtain subspectra of the CH, CH_2, and CH_3 groups, we used the sequence[21] 45°, 90°, and 135°, with an accumulation of 4096 scans.

Small-Angle X-ray Scattering (SAXS). SAXS measurements were performed on modular equipment (see ref 22 for technical details). A narrow slit was used in front of the sample to minimize the background scattering. The primary beam is narrow; the full width at half-maximum (fwhm) is 0.001 Å^{-1}. With this setup, the smallest achievable wave vector (k) is only ~0.05 Å^{-1}. The results are plotted by using $k = (4\pi/\lambda) \sin \theta$, where $\lambda = 1.542$ Å and 2θ is the scattering angle. The samples were placed in a holder between cover films of polyimide and were observed at room temperature.

Microscopy. A microscope (Nikon Labophot-2) provided with a Nikon camera (model F-601) and crossed polarizers was employed to determine the anisotropy of the samples. During these measurements, the samples were placed between a glass slide and a cover slip.

Polymerization. Two samples, named PD1 and PD2, were prepared with the same composition to examine the reproducibility of the process. They were prepared by weighing proper amounts (see Table 1) of the different components directly into a reactor that can be kept at constant temperature. To prepare the feeding mixture, the proper amount of AIBN solved in the monomer was dissolved in water, before AOT was added, followed by stirring to homogenize the mixture. The samples were then left to equilibrate at room temperature to promote the development of the two phases that were formed. To polymerize, the mixtures were kept at slightly above 60 °C for 1 day and were then allowed to cool and stay at room temperature for several days. The total mass of the samples is about 100 g. This amount is sufficient to allow the characterization of the different macroscopic phases that develop after the polymerization. Figure 2 shows the different steps followed from sample-preparation to phase-separation and final characterization.

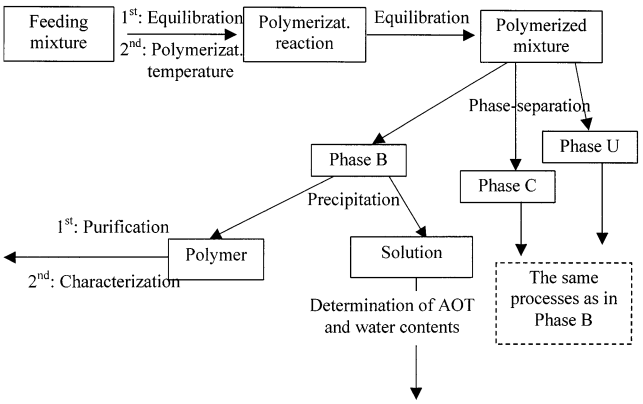

Figure 2. Scheme of the protocol followed to prepare samples and to determine the compositions of the different phases.

Table 1. Global Composition of the Samples

sample	H_2O(g) ± 0.001 (g)	DMAA(g) ± 0.0002 (g)	AOT(g) ± 0.0001 (g)	AIBN(g) ± 0.0001 (g)
PD1	67.100	8.1630	25.3047	0.0106
PD2	66.114	8.0343	25.0063	0.0111

Composition Analysis. As the concentration of the different components is high, and the total mass employed is also important, the gravimetric method gives good accuracy for all the components in the different phases.

The *in situ* synthesized PDMAA was purified to eliminate the remaining monomer, initiator, and AOT from each phase. The polymer was precipitated twice in cold acetone and later dried at 40 °C. Its ^{1}H NMR spectra showed no vinyl signals, indicating that the polymer had been purified.

Once the polymer has been separated in the first purification stage (Figure 2), the remaining liquid solution contains acetone, water, and AOT. The AOT was separated by simple evaporation of the solvents, in a rotatory evaporator, at 80 °C, under vacuum. The amount of AOT can then be determined by simple subtraction from the total mass. The amount of AOT was also determined by using an alternative spectrophotometric method with a dye for the determination of anionic surfactants (standard method ISO 7875), and the results agreed with those obtained gravimetrically.

The amount of water can then be determined by simple subtraction of AOT and PDMAA from the total mass.

Results and Discussion

Development of Phases. At the AOT concentration used here (25 wt %), the binary system AOT−water forms a single lamellar mesophase, both at room temperature and at the temperature of polymerization (Figure 1). However, experiments with DMAA added to this binary system show that this monomer induces instability of the AOT lamellar phase, and a second phase, an isotropic solution, appears with increasing DMAA concentration.[23] Thus, in the initial mixtures

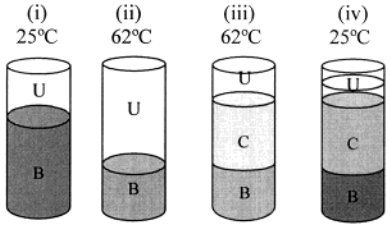

Figure 3. Qualitative description of the phases (upper, U; central, C; bottom, B) during the polymerization process: (i) starting mixture at room temperature; (ii) initial state of the polymerization immediately after the mixture is raised to the polymerization temperature; (iii) final state at the end of the polymerization, when the mixture is still at the polymerization temperature; (iv) mixture back to room temperature after the polymerization has taken place. The gray background tones denote the turbidity grades of the phases.

before polymerization, two phases can be found: an upper phase (U), which is clear and isotropic, and a bottom phase (B), which is turbid and lamellar. The situation is schematically depicted in Figure 3 as stage i. The isotropic phase U is of much smaller relative volume than the lamellar phase B. Roughly, B and U represent about $^3/_4$ and $^1/_4$ of the total volume, respectively (B occupies 78% of the total volume in PD1 and 71% in PD2, this difference resulting from small variations in the ambient temperature, to which the mixture is very sensitive). At the higher temperature in the initial state of the polymerization (slightly above 60 °C), the volume of the B phase diminishes to about $^1/_4$ (25% and 27%, for PD1 and PD2, respectively). This is depicted in Figure 3 as stage ii. An increase of the isotropic phase when the temperature is raised is expected because this is what happens in the AOT−water system without monomer, but the increase is larger here because of the presence of DMAA.[23]

During the polymerization, the volume of the bottom phase does not change much, while the upper phase evolves, yielding two phases. Thus, at the end and still at the higher temperature of the polymerization, an additional central phase (C) has appeared. This is depicted in Figure 3, as stage iii. The C phase is transparent and occupies about $^1/_2$ of the total volume (55−60%, for samples PD1 and PD2). When room temperature is recovered, and after equilibration for a long time, five (PD1) or four phases (PD2) can be obtained. This is depicted in Figure 3 as stage iv. The high number of phases after polymerization indicates that, despite the long waiting time, separation into macroscopic phases that reflect the thermodynamic equilibrium was not achieved. However, because they are macroscopic layers separated by a frontier that can be distinguished visually and they are kinetically stable, they can be called "phases", even if they do not reflect the true number of phases in thermodynamic equilibrium. The situation appears because the phases are very viscous and have only small density differences, and phases with an identical chemical composition can thus appear at many locations in the test tube. This is similar to the microscopic phase-separation and formation of "spherulites" that will be discussed below. Furthermore, it may take a rather long time until thermodynamic equilibrium is obtained between the phases in the present samples, since the transport processes become diffusion-controlled because convection and related transport phenomena are hindered because of the high viscosity.

Table 2. Compositions of the Different Phases of Samples PD1 and PD2, after Polymerization

sample	phase[a]	vol %	AOT % w/w	H_2O % w/w	PDMAA % w/w
PD1	U_1	6	9.91 ± 0.02	90.0 ± 0.2	0.11 ± 0.02
	U_2	7	18.06 ± 0.06	80.97 ± 0.01	0.976 ± 0.004
	U_3	6	13.3 ± 0.7	86.3 ± 0.8	7.84 ± 0.01
PD2	U_1	9	20.204 ± 0.008	72.87 ± 0.02	6.931 ± 0.007
	U_2	14	18.79 ± 0.05	72.33 ± 0.06	8.877 ± 0.008
PD1	C	58	21.662 ± 0.008	69.10 ± 0.01	9.238 ± 0.004
PD2	C	49	24.62 ± 0.02	66.86 ± 0.02	8.516 ± 0.008
PD1	B	25	26.34 ± 0.01	67.12 ± 0.02	6.54 ± 0.01
PD2	B	28	31.56 ± 0.01	61.94 ± 0.03	6.50 ± 0.02

[a] Upper phases (U) are numbered from lower to higher density.

Among the different phases finally obtained at room temperature after polymerization, the major ones to be considered are the bottom (B) and the next to the bottom (C) ones. Both are turbid and very viscous. Their combined volume is about 80% of the total volume, and they show no visible changes with time. The upper phases (U) are quantitatively less important, are less viscous, and seem to be in pseudoequilibrium, as we observed that, during the separation process, the phase that is extracted is partially regenerated from the others.

After the equilibration period, the different phases were separated to perform the characterization. Table 2 gathers the compositions for all phases of both samples, as determined from their analysis. The yield of polymerization was high: 92 and 95%, for samples PD1 and PD2, respectively. The B and C phases have the greater surfactant and polymer contents. Each of these two most important phases (B and C) show a similar composition for both samples (PD1 and PD2), which ensures the reproducibility of the experiment. However, in the U phases of both samples, we can find some disagreement (probably because of the sensitivity of these phases to small differences in room temperature), but this is not a hindrance for our analysis, because these U phases represent a low fraction of the total volume and most parts of the polymer and AOT are in the more reproducible B and C phases.

One can speculate on whether the polymerization starts in the initial lamellar phase or if it starts in the isotropic phase (phases B and U in stage ii of Figure 3). The answer should be that it starts in both, since the major part of the polymer appears in phases B and C at stage iv, with B being originated from the initial lamellar phase and C from the initial isotropic phase. Despite their different origins, these two final phases of stage iv present lamellar structures (as will be described below). This means that lamellae are developed by polymerization in the phase that initially was isotropic.

Let us now try to understand why so many phases appear after polymerization and why they contain lamellar structures. Figure 4 sketches the changes that occur in the phase diagram of AOT−H_2O (Figure 1). In Figure 4, only the concentration of AOT is shown, because this is the component which is responsible for the lamellar structure. When the polymerization starts (Figure 4a), the global AOT concentration, C_0, is located in a biphasic region of the diagram where the two phases that coexist are the isotropic L_1 and the lamellar L_α phases. The respective AOT concentrations in these two phases are U(ii) and B(ii) (to simplify notation, the AOT concentration in each phase is simply denoted by the symbol of the phase). The curves in Figure 4 a show

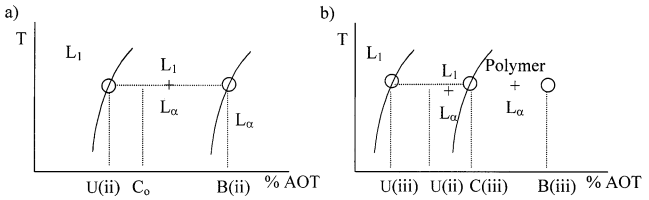

Figure 4. Qualitative concentration−temperature phase diagram of AOT, showing the relative positions of the phases (upper, U; central, C; bottom, B) at the different stages of the polymerization process (see legend of Figure 3 for their description), with respect to the regions of stability or coexistence of the lamellar (L_α) and isotropic (L_1) phases formed by AOT−water.

the coexistence of phases when the monomer DMAA is present. As we know, the presence of DMAA induces instability of the lamellar L_α phase, so that the curves of coexistence get progressively displaced toward higher AOT concentrations as DMAA is being added.[23] Hence, when DMAA is consumed in the polymerization, the coexistence curves should move to lower AOT concentrations (compare parts a and b of Figure 4).

The simultaneous appearance of polymer when monomer is consumed helps even more in this displacement of the coexistence curves toward lower AOT concentration, because (anticipating here the results that will be discussed in the next section) the polymer does not participate in the lamellar structure of AOT but segregates from it.

This shift in the macroscopic phase diagram affects the upper phase, the initial concentration of which, U(ii), is now located in a biphasic region and splits into two phases (Figure 4b). These two phases after the monomer is consumed (stage iii of Figure 3) are named U(iii) and C(iii). U(iii) is less concentrated in surfactant, so it would be isotropic, and C(iii) is the more concentrated in surfactant, so it would be lamellar (Figure 4b). In the bottom phase, B(ii), the consumption of monomer due to polymerization does not change much the AOT concentration. In fact, the volume of the B phase does not change much during polymerization and seems to be "frozen". So, at the end of the polymerization (stage iii), we have B(iii) ≅ B(ii) (Figure 4b). The B phase is already lamellar before the polymerization, and during the polymerization the decrease in monomer concentration together with the influence of the polymer synthesis is not expected to change this.

Finally, when room temperature is recovered (stage iv, Figure 3), the bottom and central phases do not change much, but the upper phase, U(iii), when at lower temperature, would be located in a region of the phase diagram where there is phase-separation, and so new phases can be formed: U_1(iv) and U_2(iv).

Microscopy. Micrographs obtained with crossed polarizers (Figure 5) show a typical marbled lamellar texture. This lamellar texture is present in all the final macroscopic phases, with the exception of U_1 from sample PD1, which is not birefringent, and U_1 from sample PD2, which presents spherulites, which are typical defects of a lamellar phase dispersed in an isotropic phase.[24,25]

Microscopy without crossed polarizers also shows that the structure of these macroscopic phases is not homogeneous. Figure 6 presents the micrographs without crossed polarizers for the phases of sample PD2. We can observe a phase-separated pattern which becomes clearer in the more dense phases, that is, in the phases with greater polymer content. The turbidity in the phases can be referred to the presence of two domains with different refractive indices, and this suggests that some phase-separation is present in the macroscopic (apparent) phases. This is similar to what happens when the preformed polymer poly(*N*,*N*-dimethylacrylamide) (PDMAA) is mixed with the lamellar phase of AOT−water. On mixing, the lamellar phase is maintained but the polymer is segregated, so there is a microscopic phase-separation in a polymer rich phase and a surfactant rich

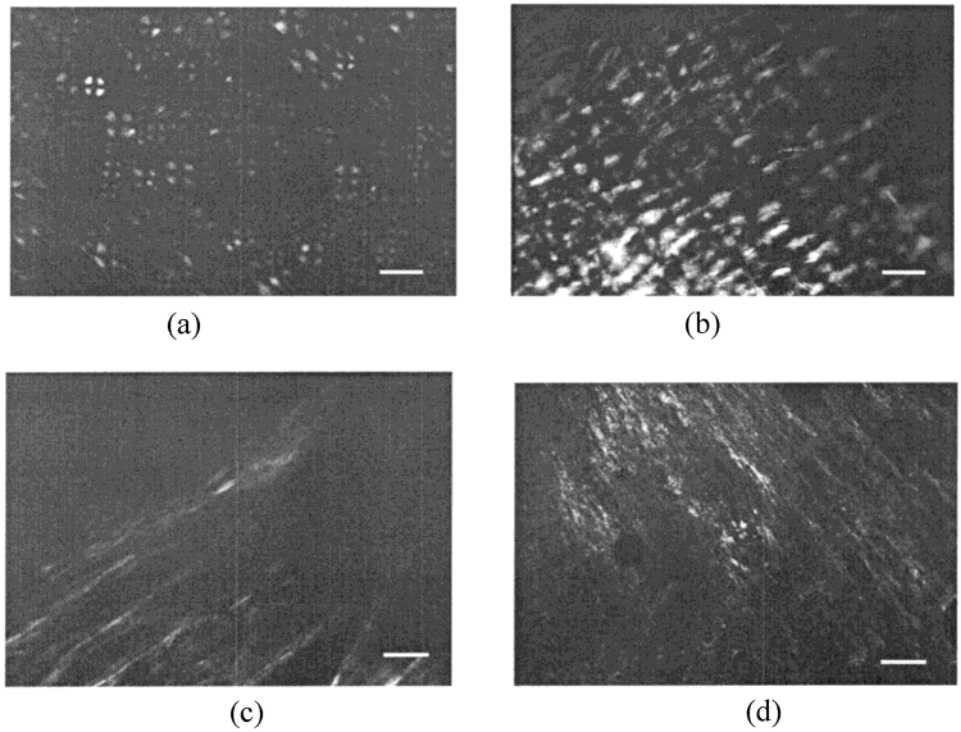

Figure 5. Micrographs with crossed polarizers from phases belonging to sample PD2: (a) U_1; (b) U_2; (c) C; (d) B. Scale: 100 μm.

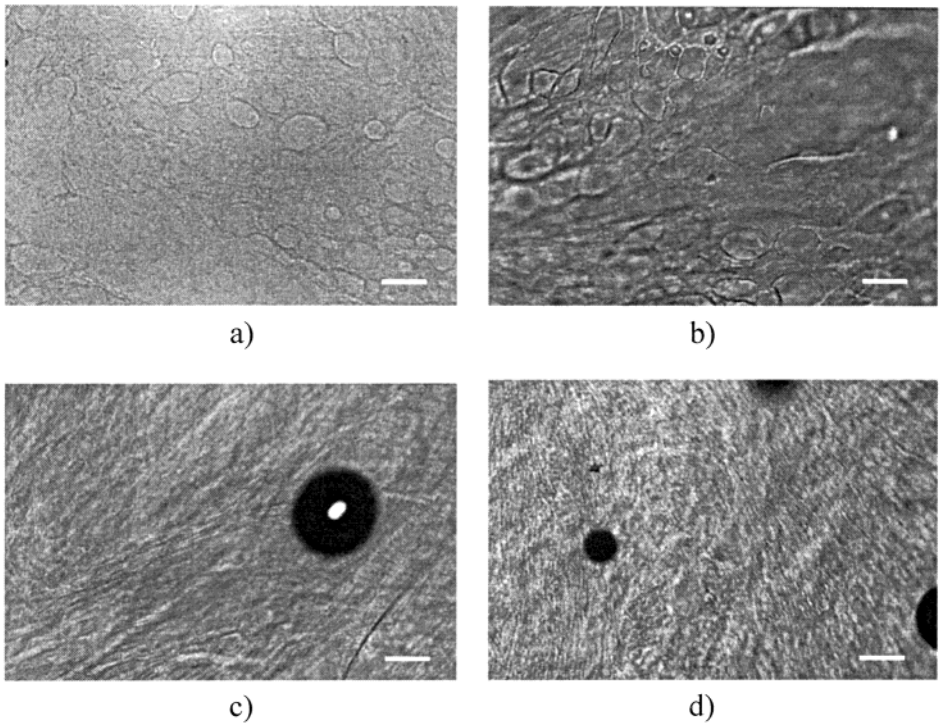

Figure 6. Micrographs without crossed polarizers from phases belonging to sample PD2: (a) U_1; (b) U_2; (c) C; (d) B. Scale: 100 μm.

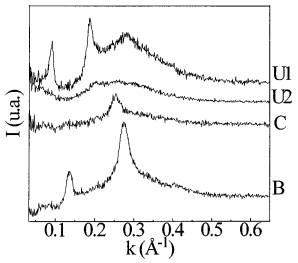

Figure 7. SAXS diffractograms for the phases in sample PD2.

phase.[26,27] We shall discuss this point more extensively below.

SAXS. Figure 7 depicts SAXS diffractograms from the different phases of sample PD2. The C and B phases were tested repeatedly during 10 months after the phases were separated, to check that their patterns did not change. All the phases show a broad hump for wave vectors between 0.1 and 0.5 $Å^{-1}$, that is characteristic of the AOT−water system.[28] Besides, there are one or several peaks with relative positions that are typical of a lamellar structure. Starting with the U phases, in U_1 there are three peaks, with *k*-values in the ratio 1:2.1:2.9, which agrees with the 1:2:3 typical ratio of a lamellar structure. In U_2, the peaks cannot be clearly seen, but this is due to the lower surfactant concentration in this phase.

Going now to the B phase, we detect two peaks, with relative positions 1:2.02, which also are in good accord with a lamellar structure. The intensity (and the fwhm, full width at half-maximum) of the first peak is lower than that of the second one. In a lamellar mesophase, the first-order Bragg peak should be the most important; usually the intensity falls off steeply for higher orders, and often with aqueous systems only the first reflection is visible. Therefore, the relative intensities of the two peaks in the B phase should be considered anomalous. It is also anomalous that in the C phase only one peak is observed. Furthermore, if we compare the *k*-position of this peak with those of the peaks in the B and U_1 phases, we would say that the peak of the C phase is not first-order but corresponds to a second-order reflection.

However, all this is reasonable in view of what is known about the AOT−water lamellar system. In AOT−water, for surfactant compositions in the range 35−45 wt %, the intensity of the first-order peak diminishes and even vanishes; at this point only the second-order peak is observable.[28] This behavior has also been detected for the PDMAA−AOT−water mixtures,[26] but in this case, the attenuation and vanishing of the first-order peak occur at lower surfactant weight fractions. The composition of the C phase agrees with the range where the first-order peak disappears in the PDMAA−AOT−water mixtures. Hence, the peak found in the C phase must be assigned to a second-order diffraction. Likewise, the attenuation of the first-order peak in the B phase is explained by the proximity of the surfactant and polymer concentrations of this phase to the range where the anomaly occurs in the PDMAA−AOT−water mixtures.

Law for the Lamellar Spacing. From the diffractograms in the small angle region presented above, we obtain information about the long range order in the lamellar system. The location of the diffraction peaks allows the determination of the long period spacing (*d*) of the lamellar structure with polymer, in each phase. Table 3 presents the experimental values of *d* from SAXS measurements. The first point to note is that *d* depends on the phase, but for a given phase, it is very similar in both samples. We have different structures depending on the phase, but not depending on the sample. The second point to note is that the lamellar spacing decreases on going from the upper to the bottom phase. Since the trend of AOT concentration is the reverse (it increases from the upper to the bottom

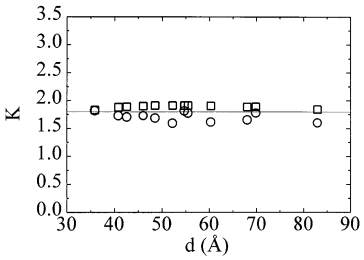

Figure 8. Partition coefficient, *K*, defined in eq 5, as a function of the lamellar spacing, *d*, for mixtures of preformed PDMAA with AOT−H_2O (different PDMAA and AOT concentrations[26,27]), calculated using $d_{AOT} = 19.6$ Å. Circles are from the experimental *d* of the mixtures; squares are from the pressures calculated theoretically for the two phases in equilibrium;[27] the line is the mean value.

Table 3. Long Period Spacing for the Lamellar Structure: *d*, Experimental Value from SAXS; d_I and d_{II}, Calculated Values from Eqs 1 and 5, Respectively (with $d_{AOT} = 19.6$ Å and $K = 1.8$)

sample	phase	*d* (Å)	d_I (Å)	d_{II} (Å)
PD2	U_1	68.9	98	64
PD1	C	51	89	55
PD2	C	52	78	52
PD1	B	44.2	75	55
PD2	B	46.2	62	48

phase), we might infer that nothing unusual occurs; that is, the spacing gets shorter as the AOT becomes more concentrated. The same thing happens in the AOT−water binary system, where the variation of *d* with AOT concentration follows the dilution law:

$$1/d = (1/d_{AOT})\varphi_{AOT} \tag{1}$$

Here, d_{AOT} is the thickness of the AOT bilayer and φ_{AOT} is the volume fraction of AOT ($\varphi_{AOT} = V_{AOT}/(V_{AOT} + V_{H_2O})$ with V_i being the total volume of component *i*).

Table 3 presents the values (d_I) calculated using eq 1, with[29] $d_{AOT} = 19.6$ Å and the volume fractions obtained from the data in Table 2 (using the densities of the components and assuming the additivity of volumes). It can be seen that there is a notable discrepancy between the calculated (d_I) and the experimental *d*-values. The experimental spacing is shorter than that predicted by eq 1. To understand this observation, we also have to take into account the third component, the PDMAA. We know that PDMAA is nonadsorbing on the surfactant film[26] and that the molecular weight of the polymer chains is such that their dimensions (see below) are too large to fit between the lamellae. Thus, from pure geometric considerations, it is expected that the polymer chains are outside the lamellar structure, and the data presented in Table 2 also suggest that the PDMAA not only segregates from the lamellae but also exerts some kind of compression on the structure. The segregated macromolecules are hydrated and should carry some water with them; that part of the total water is taken out of the lamellae. This explains the shorter spacing that is obtained when the polymer is present.

That the polymer segregates out of the lamellae and forms a (microscopically separated) isotropic phase agrees with the micrographs, where microscopic phase-separation can be detected within each macroscopic "phase". Because of the water retained by the polymer in its isotropic phase, the dilution law (eq 1) should be modified to take into account the influence of the polymer volume fraction.

We can deduce such a general law, valid in the presence of polymer, as follows. Let us divide the total volume of water, V_{H_2O}, in a purely arbitrary and formal way, in two portions: V_S and V_P ($V_{H_2O} = V_S + V_P$). Then, we define (also arbitrarily) surfactant and polymer volume fractions, φ'_{AOT} and φ'_{PDMAA}, as

$$\varphi'_{AOT} = V_{AOT}/(V_{AOT} + V_S)$$

$$\varphi'_{PDMAA} = V_{PDMAA}/(V_{PDMAA} + V_P) \tag{2}$$

We can relate these arbitrary φ's with the volume fractions experimentally determined in the phases of the samples. These experimental volume fractions are ternary variables, defined as

$$\phi_i = V_i/(V_{AOT} + V_{PDMAA} + V_{H_2O}) \tag{3}$$

with i = AOT, PDMAA, and H_2O. It is easy to show that the arbitrary and experimental volume fractions are related through

$$\phi_{AOT}/\varphi'_{AOT} + \phi_{PDMAA}/\varphi'_{PDMAA} = 1 \tag{4}$$

To connect with the lamellar spacing *d*, we assume that the system is biphasic (at the macroscopic or microscopic level) and that polymer and surfactant are separated, each in one of the phases. Because of the AOT concentration, the phase containing the surfactant is lamellar. To this lamellar phase can be applied the usual dilution law, eq 1, since the phase only contains AOT and water. Let us now specify that V_S is the volume of water that accompanies AOT in its lamellar phase. Equation 1 can be applied to this phase, and then it reads $1/d = (1/d_{AOT})\varphi'_{AOT}$. Substituting for φ'_{AOT} given by eq 4, we get

$$1/d = (1/d_{AOT})(\phi_{AOT} + K\phi_{PDMMA}) \tag{5}$$

where $K = \varphi'_{AOT}/\varphi'_{PDMAA}$. If *K* is constant, then eq 5 is a general dilution law which expresses the reciprocal spacing proportional to both the surfactant and polymer volume fractions.

We now contend that *K* is effectively constant. Thermodynamically, *K* is related to a partition coefficient. Since water is being partitioned between the surfactant and polymer phases, the ratio of water concentrations in the two phases, $(1 - \varphi'_{AOT})/(1 - \varphi'_{PDMAA})$, is a partition coefficient. Experimental and theoretical data previously obtained can be used to show that *K* is constant. When preformed PDMAA was mixed with AOT−water, the experimental spacing could be fitted to the equation[27]

$$1/d = 0.051\phi_{AOT} + 0.090\phi_{PDMMA}\ (\text{Å}^{-1}) \tag{6}$$

which is equivalent to eq 5 with $d_{AOT} = 19.6$ Å and a constant *K* ($K = 1.8$). In Figure 8 are shown the values of *K* calculated with eq 5 when applied to the previous results of *d* for the PDMAA−AOT−H_2O mixtures.[26,27] They correspond to different AOT and PDMAA concentrations that cover a wide range of *d* spacings (encompassing those found here). We can see that the calculated *K* has no trend with *d* and fluctuates around a constant value ($K = 1.7$).

Another test for the constancy of *K* is obtained using previous theoretical calculations of the osmotic pressure in each of the two phases: AOT−water and PDMAA−

Table 4. Intrinsic Viscosity, [η], of Polymer PDMAA Found in the Different Phases of Samples PD1 and PD2 after Polymerization

sample	phase	[η] (dL/g)
PD1	U_3	4.38[a]
PD2	U_1	4.77[a]
	U_2	4.50[a]
PD1	C	4.61,[a] 4.47,[b] 4.49[c]
PD2	C	4.06[a]
PD1	B	4.26[a]
PD2	B	4.43[a]

[a] [η] determined in [$NaNO_3$] = 0.1 M, at 30 °C. [b] [η] determined in water, at 25 °C. [c] [η] determined in methanol, at 25 °C.

water. If these two phases are in equilibrium, the chemical potential of water has to be the same in both. Hence, their osmotic pressures have to be equal. The osmotic pressure in the lamellar phase only depends on φ'_{AOT}, and the osmotic pressure in the isotropic phase only depends on φ'_{PDMAA}. The value of K is determined by the φ'_{AOT} and φ'_{PDMAA} values that make the two pressures equal. In Figure 8 are shown the values of K that are calculated from the equality of osmotic pressures, using for these osmotic pressures their corresponding theoretical expressions.[27] As can be seen, this calculated K is also practically constant ($K = 1.9$). In conclusion, different methods give a K which remains effectively constant over a wide range of lamellar spacings covering different AOT and PDMAA concentrations, and the mean value obtained from these various methods is $K = 1.8$.

We can now calculate the spacing predicted by the theoretical eq 5, with $d_{AOT} = 19.6$ Å and $K = 1.8$, for the phases of the present samples polymerized *in situ*. Table 3 shows the results of this calculation (d_{II}). We can see that these theoretical d values (d_{II}) agree much better with the experimental d than the previous ones (d_I), and we conclude that eq 5 is a good representation of the law that describes the contraction of the AOT lamellar spacing as a function of surfactant and polymer concentration, and that the same parameter values deduced from the mixing of preformed polymer with surfactant are valid here where the polymer has been polymerized *in situ*. The compliance with eq 5 is in agreement with the model of segregation of the polymer from the lamellae to an isotropic microphase, from which it exerts an osmotic compression on the lyotropic mesophase that reduces the lamellar spacing.

Polymer Size. The intrinsic viscosity ([η]), determined for solutions of the polymer separated from the different phases of samples PD1 and PD2, is shown in Table 4. We can see that the results for the two samples (PD1 and PD2) and the different phases are very similar. For example, those measured in [$NaNO_3$] = 0.1 M, at 30 °C, for all the phases, lie within the narrow range 4.1−4.8 dL/g. This means that the polymers are formed with very similar molecular weights in all the phases. In other words, the macromolecular size is not significantly dependent on the AOT concentration or the mesophase structure of the medium (in the conditions used here). By using the Mark−Houwink equation in water,[30] with the exponent $a = 0.81$ and the constant $K = 2.24 \times 10^{-5}$ dL/g, the value calculated for the viscous molecular weight average is $\overline{M_v} = 3.4 \times 10^6$ g/mol, which is similar to that obtained for a polymer synthesized in pure water.[26] Thus, AOT has not modified the chain length usually attained in this type of polymerization.

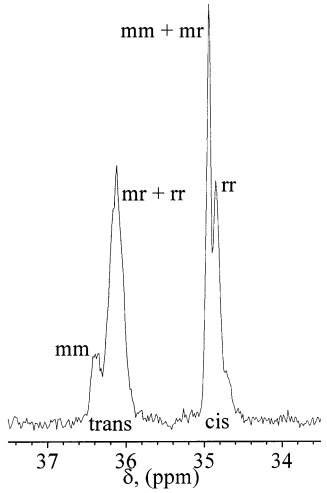

Figure 9. Edited ^{13}C NMR spectrum, obtained with a DEPT sequence, showing the region of the lateral CH_3 groups of PDMAA, for the polymer recovered from phase B of sample PD1.

Polymer Tacticity. ^1H and ^{13}C NMR spectra have been recorded for the different polymers extracted from phases B and C of the two samples PD1 and PD2. ^1H spectra are similar in all the phases and also similar to that of another PDMAA synthesized in water. The ^{13}C spectra for the carbonyl signal are also very similar for the polymers obtained from the phases and for a PDMAA synthesized in water. But for the purpose of analyzing whether the mesophase has exerted some influence on the microstructure of the polymer formed, the carbonyl signal is not very sensitive.[20] The signal of the lateral methyl groups is more sensitive to steric composition. Unfortunately, because of the overlap with the main chain carbons, the analysis of N−CH_3 by means of the conventional carbon spectrum is unsuccessful. Nevertheless, the DEPT sequences enable us to analyze the stereochemical structure of this polymer.[20]

With the DEPT sequence detailed in the Experimental Section we can obtain the spectrum corresponding to the carbon atoms in the $N(CH_3)_2$ groups. The combination of subspectra for 45°, 90°, and 135° (named subspectra $S(1)$, $S(2)$, and $S(3)$, respectively) gives the desired signal of $N(CH_3)_2$ carbons, $S(CH_3)$, as[21]

$$S(CH_3) = S(1) + S(3) - 1.414S(2) \qquad (7)$$

The edited spectrum resulting from this combination is illustrated in Figure 9 for one of the polymers. The spectrum consists of two bands which correspond to the two possible configurations, *cis* and *trans*, of the N-bonded CH_3 groups. From the relative areas of these two bands, we obtain the fractions of the corresponding configurations. Table 5 shows the results for the polymers recovered from the two main phases, B and C, of the two samples polymerized *in situ* (PD1 and PD2) and also for the polymer synthesized in pure water. We can see that this combination of spectra gives practically the same fraction of *cis* and *trans* configurations in all cases.

The microtacticity of these polymers can then be obtained from the peaks in each band. These peaks are assigned to triad configurations: isotactic (mm), syndiotactic (rr), and heterotactic (mr), following the assignment made before.[20] This is shown in Figure 9. The fractions of the different triads, determined from these

Table 5. Microstructure[a] of the Polymers Recovered from Phases B and C (Samples PD1 and PD2), Compared with that of a PDMAA Synthesized in Pure Water

	%	triads			diads	
polymer	*trans*	mm	mr	rr	m	r
water	51	0.16	0.42	0.42	0.37	0.63
phase C PD1	50	0.17	0.39	0.44	0.36	0.64
phase B PD1	51	0.17	0.30	0.53	0.32	0.68
phase C PD2	50	0.18	0.36	0.46	0.36	0.64
phase B PD2	51	0.16	0.45	0.39	0.38	0.62

[a] Configuration of the CH_3 groups bonded to N (*trans* fraction) and microtacticity: fraction of isotactic (mm), syndiotactic (rr), and heterotactic (mr) triads and fraction of meso (m) and racemic (r) diads. Results are calculated from the $N(CH_3)_2$ signal in the ^{13}C NMR spectrum with a DEPT sequence.

peak areas in the combined DEPT spectra, are shown in Table 5. From these triads we also calculate the diad fractions: meso (m) and racemo (r). We can see that the polymers are predominantly racemo, with greater proportion of syndio and hetero triads, something which is expected for the type of initiator and monomer used.

When comparing the different polymers, no clear distinction between the tacticities of those from phases B or C can be seen. Moreover, no clear distinction in tacticities between the polymers synthesized *in situ* and the polymer synthesized in pure water can be seen either. Hence, we can conclude that the microstructures of PDMAA polymerized *in situ* and in pure water are similar. This means that the lamellar structure of the mesophase had no influence on the microstructure of the polymer formed *in situ*. To get a template effect, other conditions different from those prevailing here should be attained. Among possible adverse circumstances, the present lamellar spacings may be too large for a true confinement of the propagating unit, and the growing chain can also perhaps segregate from the lamellar structure in the early stages of propagation.

Conclusions

The splitting of the monomer-containing biphasic mixture into more phases after polymerization is understandable in terms of the evolution of the system within the AOT−water phase diagram. These arguments also allow us to understand that the final phases are anisotropic and contain a lamellar structure, although some have originated from an isotropic phase. The large number of phases that are observed in the samples after polymerization is not expected to reflect the number of phases that are in thermodynamic equilibrium, whereas a high viscosity minimizes convection and slows down the evolution of macroscopically separated phases which otherwise may have formed because of density differences.

The microheterogeneous nature of the macroscopic (apparent) phases is explained because the polymer formed *in situ* segregates from the lamellar structure. The spacing of the lamellar AOT−water structure is shortened by the segregated polymer, which exerts an osmotic compression on the lamellae, similar to that observed for AOT−water mixed with preformed polymer. The law that expresses the change in lamellar spacing with polymer concentration can be deduced from the equilibrium between the surfactant and polymer microphases.

The polymerization in this lyotropic medium yields polymers having the same molecular weight and tacticity as a polymer synthesized in pure water. Thus, no template effect of the lamellar mesophase on the polymer takes place at these lamellar spacings.

Acknowledgment. We gratefully acknowledge Profs. Olli Ikkala (Department of Engineering Physics and Mathematics, Helsinki University of Technology, Finland) and Mika Torkkeli (Department of Physical Sciences, University of Helsinki, Finland) for the SAXS determinations and for their hospitality and helpful advice given to I.E.P. during her visiting stay. Financial support from CICYT, Spain (Grant BQU2000-0251), and from UNED is gratefully acknowledged.

References and Notes

(1) Guymon, C. A.; Hoggan, E. N.; Clark, N. A.; Rieker, T. P.; Walba, D. M.; Bowman, C. N. *Science* **1997**, *257*, 57−59.
(2) Guymon, C. A.; Bowman, C. N. *Macromolecules* **1997**, *30*, 5271−5278.
(3) Antonietti, M.; Bremser, W.; Müschenborn, D.; Rosenauer, C.; Schupp, B. *Macromolecules* **1991**, *24*, 6636−6643.
(4) Renken, A.; Hunkeler, D. *Polymer* **1999**, *40*, 3545−3554.
(5) Anderson, D. M.; Ström, P. *Langmuir* **1992**, *8*, 691−709.
(6) Jung, M.; German, A. L.; Fischer, H. R. *Colloid Polym. Sci.* **2000**, *278*, 1114−1118.
(7) Jung, M.; German, A. L.; Fischer, H. R. *Colloid Polym. Sci.* **2001**, *279*, 105−113.
(8) Demé, B.; Dubois, M.; Zemb, T.; Cabane, B. *J. Phys. Chem.* **1996**, *100*, 3828−3838.
(9) Antonietti, M.; Caruso, R. A.; Hentze, H. P.; Göltner, C. *Macromol. Symp.* **2000**, *152*, 163−172.
(10) Herz, J.; Husson, F. R.; Rempp, P.; Luzzati, V. *J. Polym. Sci.* **1964**, Pt. C (No. 4), 1275−1290.
(11) Friberg, S. E.; Thundatil, R.; Stoffer, J. O. *Science* **1979**, *205*, 607−608.
(12) Holtscherer, C.; Wittman, J. C.; Guillon, D.; Candau, F. *Polymer* **1990**, *31*, 1978−1985.
(13) Hentze, H. P.; Göltner, C. G.; Antonietti, M. *Ber. Bunsen-Ges Phys. Chem.* **1997**, *101*, 1699−1997.
(14) Hentze, H. P.; Antonietti, M. *Curr. Opin. Solid State Mater. Sci.* **2001**, *5*, 343−353.
(15) Candau, F.; Leong, Y. S.; Fitch, R. M. *J. Polym. Sci.* **1985**, *23*, 193−214.
(16) Lester, C. L.; Colson, C. D.; Guymon, C. A. *Macromolecules* **2001**, *34*, 4430−4438.
(17) Renken, A.; Hunkeler, D. *Polymer* **1999**, *40*, 3545−3554.
(18) Winsor, P. A. In *Liquid Crystals and Plastic Crystals*; Gray G. W., Winsor, P. A., Eds.; Ellis Horwood Limited: Chichester, 1974: Vol. 1, p 205.
(19) Soltero, J. F. A.; Robles-Vázquez, O.; Puig, J. E. *J. Rheol.* **1995**, *39* (1), 235−240.
(20) Bulai, A.; Jimeno, M. J.; Alencar de Queiroz, A.; Gallardo, A.; San Román, J. *Macromolecules* **1996**, *29*, 3240−3246.
(21) Günther, H. *NMR Spectroscopy*, 2nd ed.; John Wiley & Sons: Chichester, 1995; p 475.
(22) Brinke, G.; Ikkala, O.; Ruokolanien, J.; Torkkeli, M.; Serimaa, R.; Vahvasellkä, S.; Saariaho, M. *Macromolecules* **1996**, *29*, 6621−6628.
(23) Pacios, I. E.; Renamayor, C. S.; Horta, A.; Lindman, B.; Thuresson, K. *Colloid Surf., A*, submitted.
(24) Porte, G.; Appel, J.; Bassereau, P.; Marignan, J. *J. Phys. Fr.* **1989**, *50*, 1335−1347.
(25) Hartshorene, N. H. In *Liquid Crystals and Plastic Crystals*; Gray, G. W., Winsor, P. A., Eds.; Ellis Horwood Limited: Chichester, 1974; Vol. 2, p 57.
(26) Pacios, I. E.; Lindman, B.; Horta, A.; Thuresson, K.; Renamayor, C. S. *Colloid Polym. Sci.* **2002**, *280*, 517−525.
(27) Pacios, I. E.; Renamayor, C. S.; Horta, A.; Lindman, B.; Thuresson, K. *J. Phys. Chem. B* **2002**, *106*, 5035−5041.
(28) Nallet, F.; Laversanne, R.; Roux, D. *J. Phys. II* **1993**, *3*, 487−502.
(29) Fontell, K. *J. Colloid Interface Sci.* **1973**, *44*, 318−329.
(30) Trossarelli, L.; Meirone, M. *J. Polym. Sci.* **1962**, *23*, 445−452.

MA020724Q